Electronic Supplementary Information (ESI)

Solvent-induced surface hydroxylation of layered perovskite Sr$_3$FeCoO$_{7-\delta}$ for enhanced oxygen evolution catalysis

Kongliang Xu[+,1,2], Fang Song[+,2,*], Jun Gu[2], Xiang Xu[2], Zhenning Liu[1,*], Xile Hu[2,*]

1 Key Laboratory of Bionic Engineering (Ministry of Education), College of Biological and Agricultural Engineering, Jilin University, Changchun, Jilin 130022, P. R. China. Correspondence and requests for materials should be addressed to Z. L. (email: liu_zhenning@jlu.edu.cn)

2 Laboratory of Inorganic Synthesis and Catalysis, Institute of Chemical Sciences and Engineering, École Polytechnique Fédérale de Lausanne (EPFL), EPFL-ISIC-LSCI, BCH 3305, Lausanne 1015 Switzerland. Correspondence and requests for materials should be addressed to F.S. (email: sofa0318@gmail.com) or to X.H. (email: xile.hu@epfl.ch)

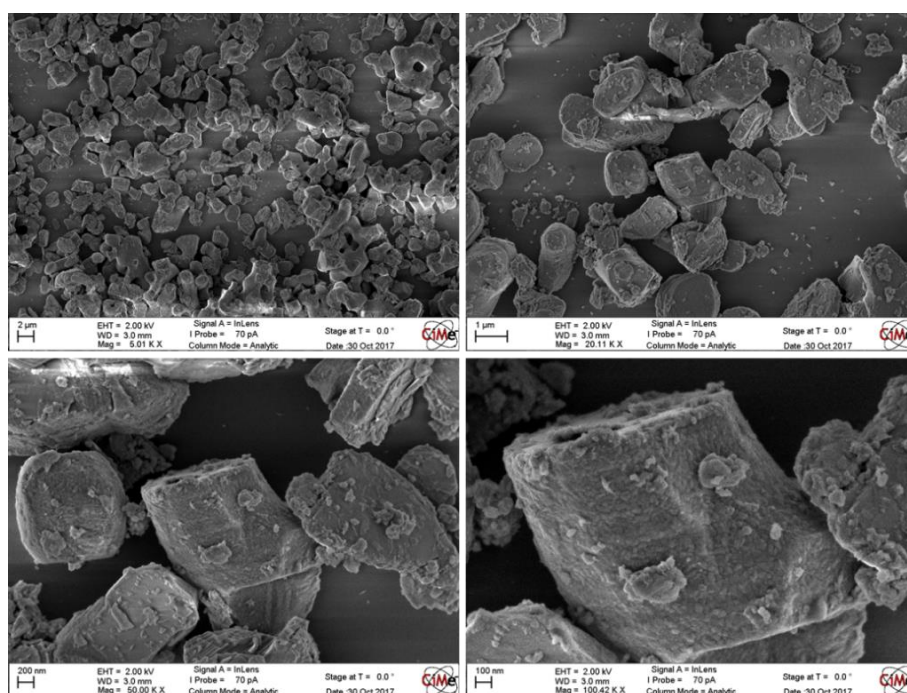[+] These authors contributed equally to this work.

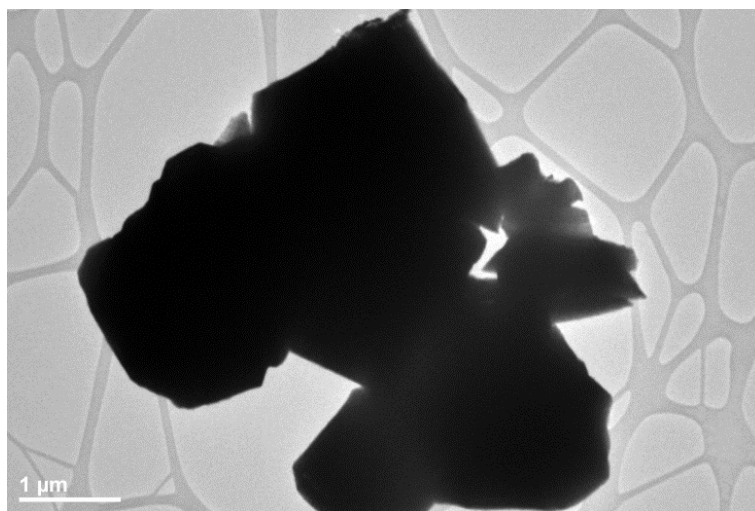**Fig. S1** SEM images of untreated layered perovskite Sr$_3$FeCoO$_{7-\delta}$

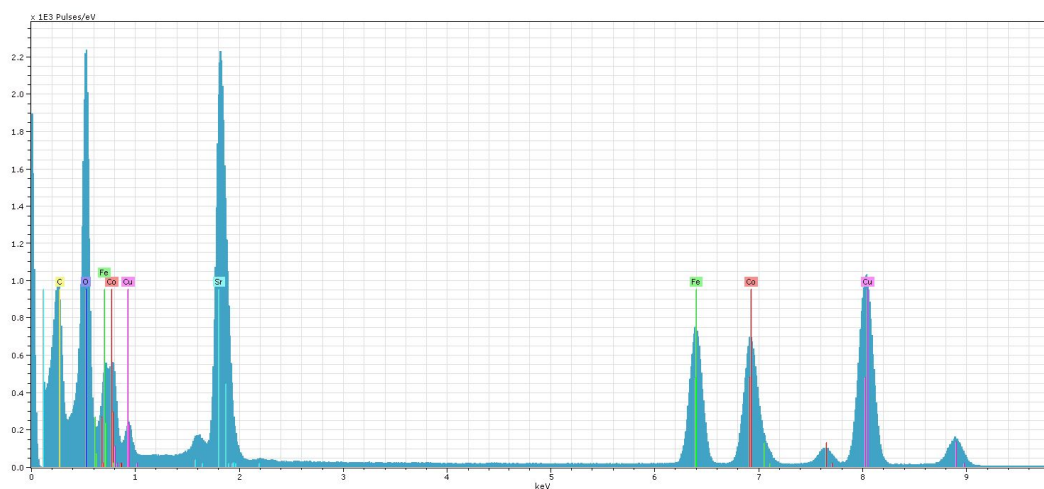**Fig. S2** TEM image of untreated layered perovskite $Sr_3FeCoO_{7-\delta}$.

Fig. S3 EDX pattern of untreated layered perovskite $Sr_3FeCoO_{7-\delta}$, with the ratio of Sr:Fe:Co as 3.2:1.1:1. EDX pattern were taken on a FEI Tecnai Osiris TEM under a scanning TEM modal. The elemental ratio was calculated from the Kα peak area of each element, using the software of ESPRIT 2 (Bruker).
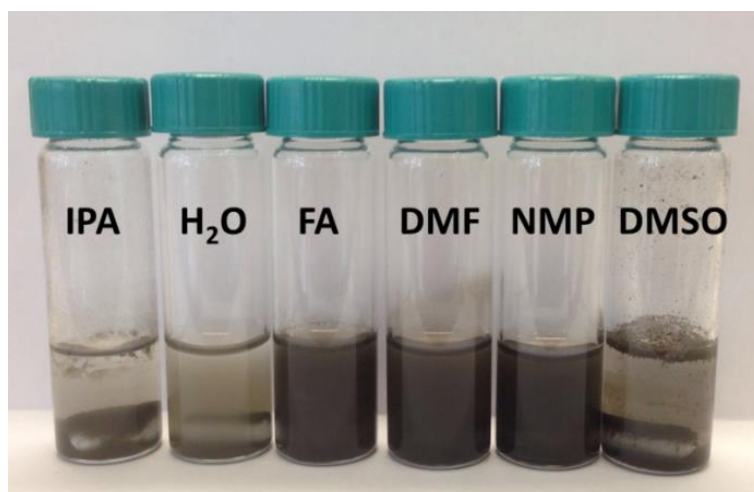
Fig. S4 Photograph of hydroxylated layered perovskite $Sr_3FeCoO_{7-\delta}$ with different solvent treatments, indicating the delamination is failed.

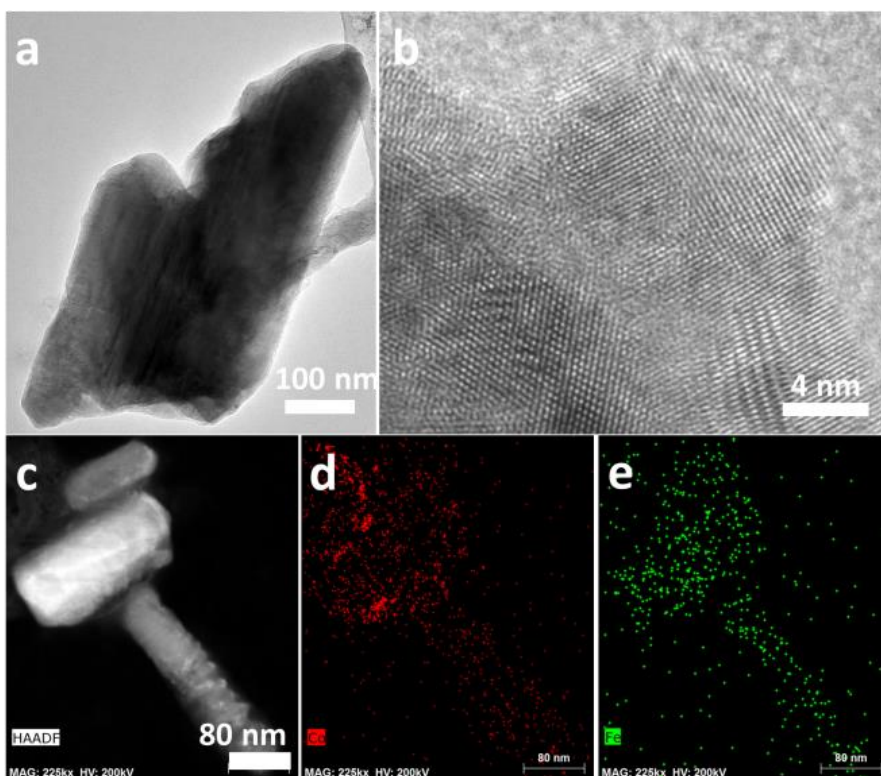**Fig. S5** (HR-)TEM images, HAADF and EDX mapping images of NMP-treated $Sr_3FeCoO_{7-\delta}$ post-OER electrolysis: (a) TEM image; (b) HR-TEM image; (c) HAADF image and corresponding elemental mapping images of (d) Co and (e) Fe.

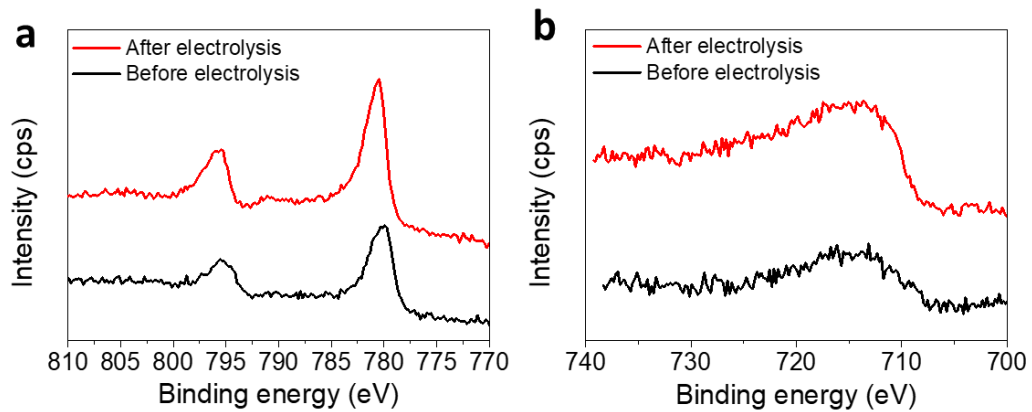**Fig. S6** High resolution XPS spectra of (a) Co_{2p} and (b) Fe_{2p} for NMP-treated $Sr_3FeCoO_{7-\delta}$ before and after OER catalysis.

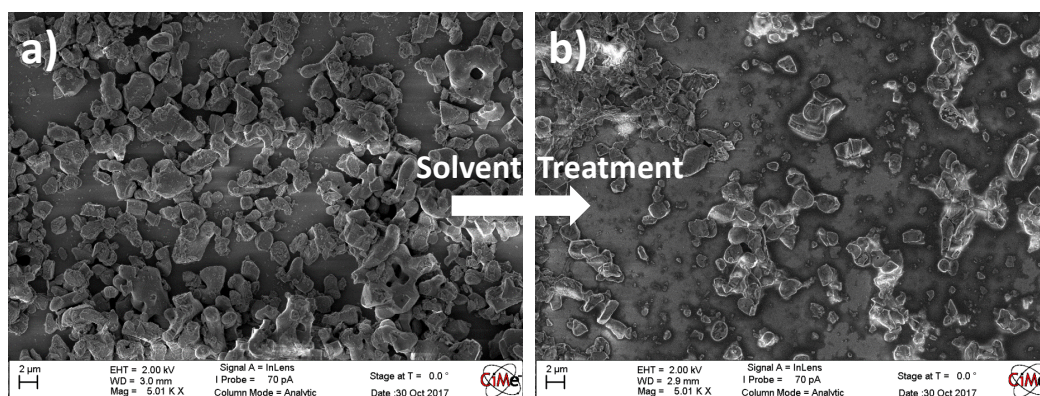**Fig. S7** Comparison of SEM images of untreated and NMP-treated hydroxylated layered perovskite $Sr_3FeCoO_{7-\delta}$
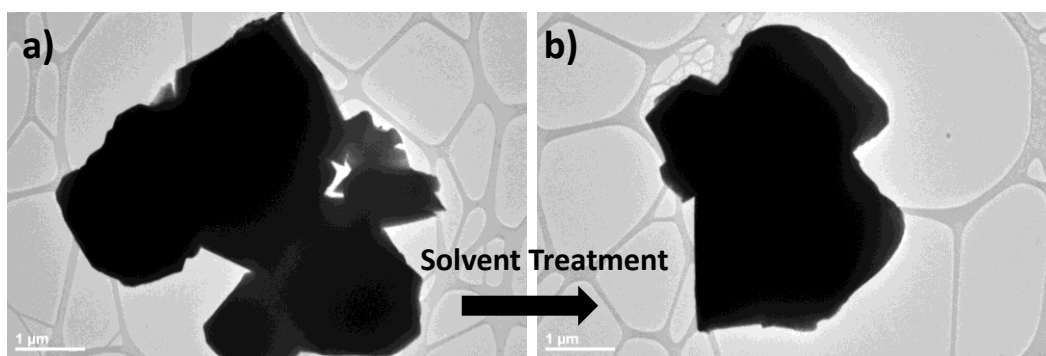
Fig. S8 Comparison of TEM images of untreated (a) and NMP-treated (b) hydroxylated layered perovskite $Sr_3FeCoO_{7-\delta}$
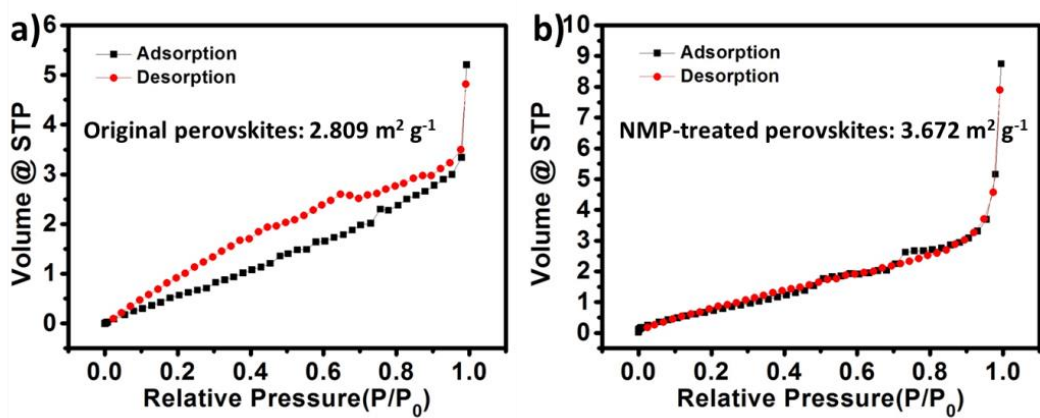
Fig. S9 Comparison of N_2 adsorption-desorption measurement.
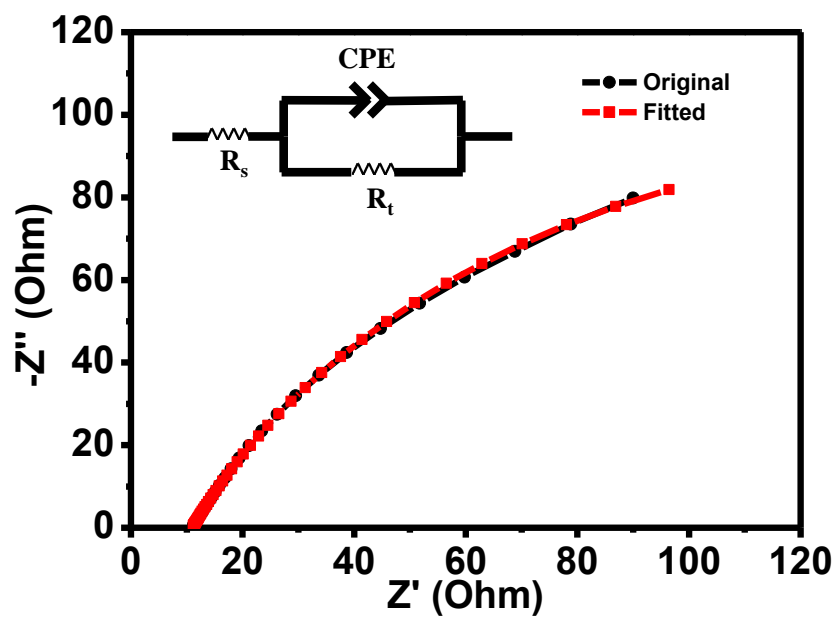
Fig. S10 Nyquist plots for layered perovskite of 4-day NMP treatment (Black line for original data, red line for fitted data); the inset is the corresponding equivalent circuit model.

Fig. S11 Thermogravimetric analysis of NMP-treated perovskites and vacuum dried NMP-treated perovskites.

Fig. S12 XRD pattern of NMP-treated perovskites after vacuum drying

Fig. S13 Polarization curves of untreated, NMP-treated, vacuum dried NMP-treated perovskites.

Fig. S14 XRD patterns of NMP-treated perovskites prepared from different methods. For the solid powder, the perovskites were dried and grinded (destroy the preferred o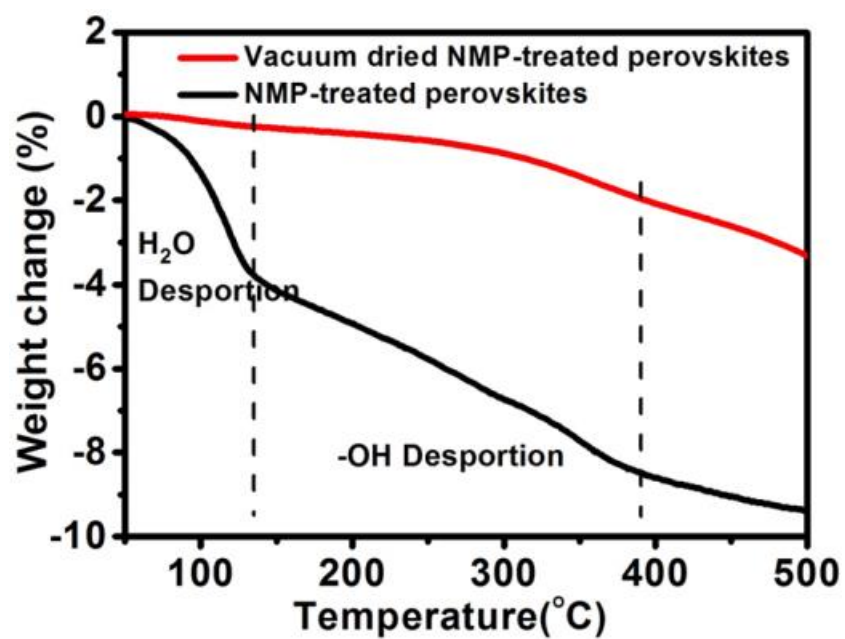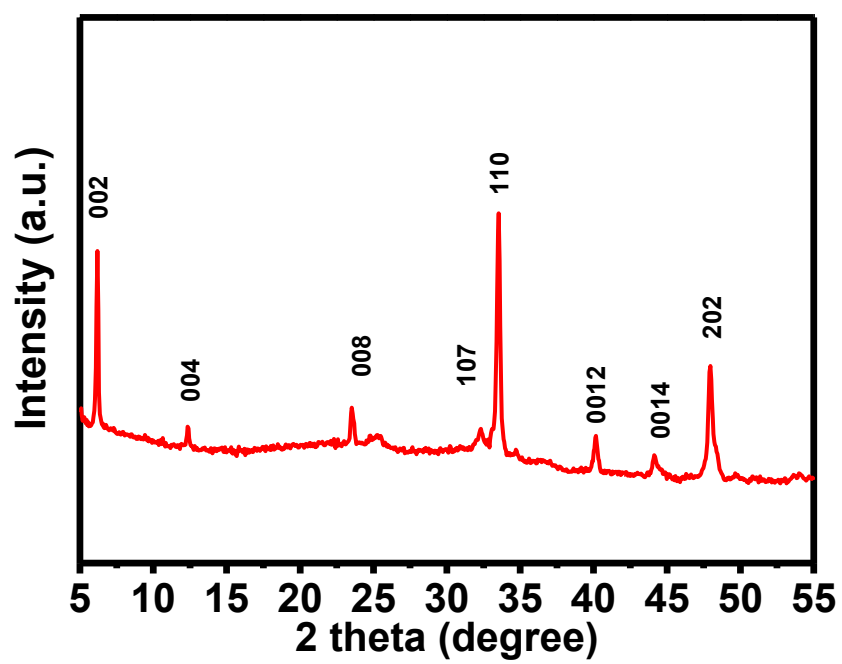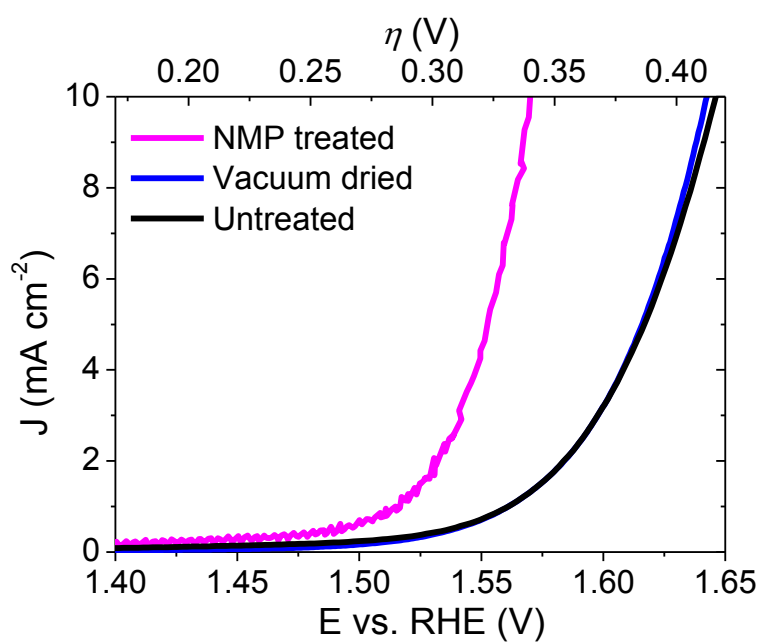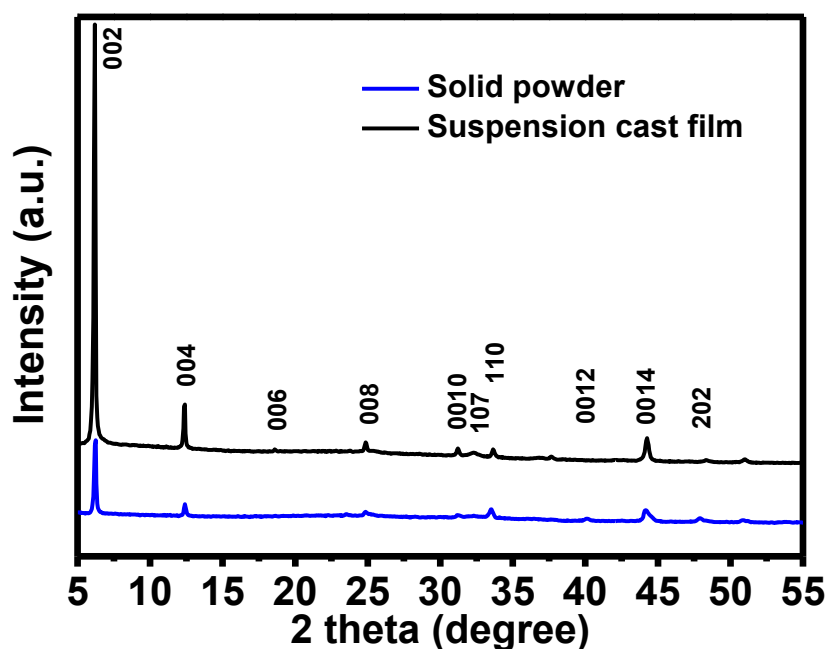rientation), and pressed on the glass substrate to form a plane for XRD characterization. For suspension cast film, the perovskites with alcohol were directly dried on glass substrate at room temperature and then used for XRD characterization. The lower (002) intensity of solid powder compared to suspension cast film (suspension cast film > solid powder > untreated sample) suggests both bulk hydroxylation and preferred orientation contribute to the large $R_{002/110}$ of suspension cast film.

It is reasonable to use the relative intensity of $R_{002/110}$ as a semi-quantitative index to evaluate the degree of hydroxylation for Ruddlesden-Popper type perovskites oxides. This was supported by the previously reported result that the hydroxylation of perovskites increases the intensities of the peaks corresponding to the planes of (00n) (n=2, 4, 6, 8, 10, 12 and 14), while remains unchanged intensities for the (110) plane (*Chem. Mater.*, 2005, 17, 773). Although our XRD measurement with solid powder (no preferred orientation, Fig. S14) showed that the high (002) intensity was partially ascribed to the preferred (00n) orientation of suspension cast film (Fig. S14), this will not impair the validity of using $R_{002/110}$ as the semi-quantitative index. The reason is that the preferred (00n) orientation was exactly induced by the surface hydroxyl groups (the product of hydroxylation). The hydroxyl groups induced preferred orientation is shown in Fig. S15 (c, d). Similar preferred orientation was previously demonstrated for layered double hydroxides when they were dried from the suspension (*J. Am. Chem. Soc.*, 2006, 128, 8376-8377). Higher content of surface hydroxyl groups would lead to higher degree of preferred orientation. In this sense, the $R_{002/110}$ of suspension cast film reflects well on the degree of hydroxylation.
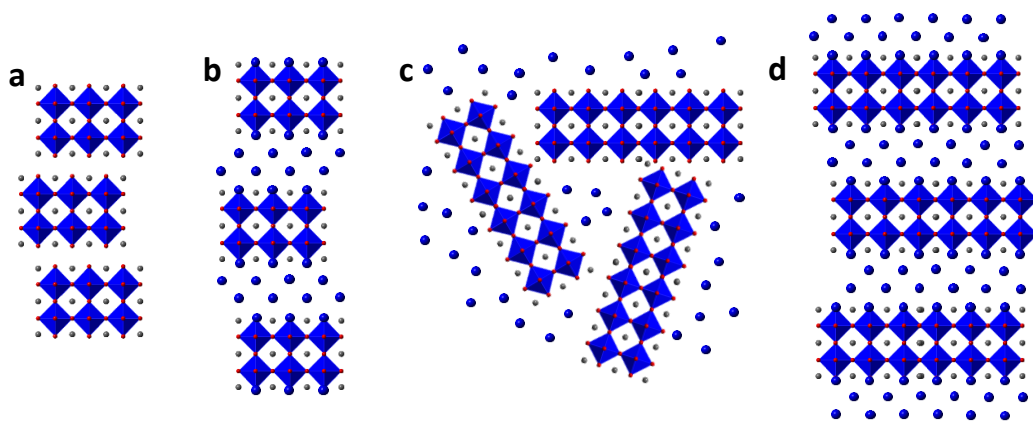
Fig. S15 a, b) Crystal structure of dehydroxylated (a) and fully hydroxylated (b) layered perovskites; c) accumulation of dehydroxylated layered perovskites during the drying process. For simple illustration, each layer represents one particle. d) self-assembly of hydroxylated layered perovskites. For simple illustration, each layer represents one particle. Color code: Yellow brown spheres for OH; Green spheres for H_2O.

Fig. S15a shows the crystal structures of dehydroxylated layered perovskites. The layers are linked by strong chemical bonding. When we consider the particle surface in the drying process, chemical bonding are hard to be formed between the particles and thus the particles cannot be stacked in order (Fig. S15c).

In contrast, the layers in hydroxylated samples are linked by the hydrogen bonding between intercalated H_2O molecules and OH groups. When we consider the particle surface in this drying process, the hydroxylated surface likely drive the particles to assemble in order, as shown in Fig. S15d. The ordered stacking resulted in the strong XRD peak of (00n), which corresponds to the hydroxylated layers.
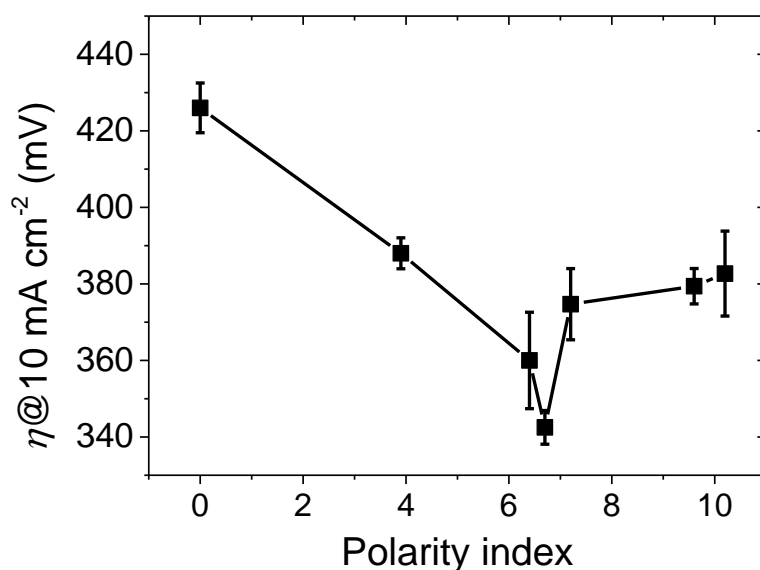
Fig. S16 Overpotential (at 10 mA cm^{-2}) plotting against the polarity index of solvents used in the treatment of layered perovskite $Sr_3FeCoO_{7-\delta}$.

The different degree of surface hydroxylation might be ascribed to the different polarity of solvents. The solvent might have two effects on the perovskite surface: 1) affecting the contact between water molecules and perovskite oxide surface; 2) affecting the hydroxylation reaction between them. Normally, the surface of perovskites is moderately hydrophobic (J. Phys. Chem. C 2015, 119, 18504). Solvents with lower polarity than water (polarity index: 10.2) can facilitate the contact with perovskite oxide surface (hydrophobic), while the hydroxylation reaction might be restricted with extremely low polarity solvents due to the large polarity contrast between water and solvents. This is consistent with our result that an optimized catalytic activity was observed for the solvent with a medium polarity.

Table S1 Comparison of perovskite catalysts in the literatures.

Catalysts	Substrate	Additives	Overpotential (mV) at 10mA cm^{-2}	Tafel slope (mV dec^{-1})	ref.
NMP-treated $Sr_3FeCoO_{7-\delta}$	Glassy carbon	CNT	343	62.6	Our work
Original $Sr_3FeCoO_{7-\delta}$	Glassy carbon	CNT	426	76.9	Our work
$LaFeO_3$	Glassy carbon	conductive carbon	500	77	1
$La_{0.95}FeO_{3-\delta}$	Glassy carbon	conductive carbon	400	48	1
$Ba_{0.5}Sr_{0.5}Co_{0.8}Fe_{0.2}O_{3-\delta}$	Glassy carbon	acetylene black	370	60	2
$SrFeO_3$	Glassy carbon	acetylene black	410	63	3
$CaFeO_3$	Glassy carbon	acetylene black	390	47	3
$CaCu_3Fe_4O_{12}$	Glassy carbon	acetylene black	400	51	3
$LaCo_{0.8}Fe_{0.2}O_3$	Nickel foam	none	350	59	4
$Sr_2Fe_{1.3}Ni_{0.2}Mo_{0.5}O_{6-\delta}$	Glassy carbon	none	360	59	5
$LaSr_3Co_{1.5}Fe_{1.5}O_{10-\delta}$	Glassy carbon	carbon black	388	83.9	6
$SrNb_{0.1}Co_{0.7}Fe_{0.2}O_{3-\delta}$	Glassy carbon	conductive carbon	420	76	7

Reference

1   Y. L. Zhu, W. Zhou, J. Yu, Y. B. Chen, M. L. Liu and Z. P. Shao, *Chem. Mater.*, 2016, **28**, 1691-1697.

2   J. Suntivich, K. J. May, H. A. Gasteiger, J. B. Goodenough and Y. Shao-Horn, *Science*, 2011, **334**, 1383.

3   S. Yagi, I. Yamada, H. Tsukasaki, A. Seno, M. Murakami, H. Fujii, H. Chen, N. Umezawa, H. Abe, N. Nishiyama and S. Mori, *Nat. Commun.*, 2015, **6**.

4   B. Q. Li, C. Tang, H. F. Wang, X. L. Zhu and Q. Zhang, *Sci. Adv.*, 2016, **2**.

5   K. Zhu, T. Wu, M. Li, R. Lu, X. Zhu and W. Yang, *J. Mater. Chem. A*, 2017, **5**, 19836-19845.

6   S. Liu, H. Luo, Y. Li, Q. Liu and J.-L. Luo, *Nano Energy*, 2017, **40**, 115-121.

7   Y. Zhu, W. Zhou, Z.-G. Chen, Y. Chen, C. Su, M. O. Tadé and Z. Shao, *Angew. Chem. Int. Ed.*, 2015, **54**, 3897-3901.

Table S2 The double layer capacitance, roughness and specific current density of the layered perovskite catalysts.

Layered perovskite	C_{dl} ($\mu F\ cm^{-2}$)[a]	Roughness[b]	$J_{s@350\ mV}$ ($mA\ cm^{-2}$)
0-day treatment	48.1	0.60	2.16
1-day treatment	100.5	1.26	1.69
2-day treatment	118.9	1.49	2.81
4-day treatment	127.4	1.59	6.29

a: the double layer capacitance associated with the CPE was calculated according to equation: $C_{dl} = Q^{1/\alpha}$ $(R_e^{-1} + R_t^{-1})^{(\alpha-1)/\alpha}$. b: the roughness was calculated by considering the specific capacitance $C_s = 80\ \mu F cm^{-2}$.